Radiotherapy and Oncology 165 (2021) 159–165

Contents lists available at ScienceDirect

Radiotherapy and Oncology

journal homepage: www.thegreenjournal.com

Original Article

# Can the mean linear energy transfer of organs be directly related to patient toxicities for current head and neck cancer intensity-modulated proton therapy practice?

Dirk Wagenaar [a,*], Ewoud Schuit [b], Arjen van der Schaaf [a], Johannes A. Langendijk [a], Stefan Both [a]

[a] Department of Radiation Oncology, University Medical Center Groningen, University of Groningen; and [b] Julius Center for Health Sciences and Primary Care, University Medical Center Utrecht, Utrecht University, Utrecht, the Netherlands

ARTICLE INFO

*Article history:*
Received 11 March 2021
Received in revised form 5 August 2021
Accepted 4 September 2021
Available online 14 September 2021

*Keywords:*
Proton beam therapy
Biological modeling
Head and neck tumors
NTCP modeling
Relative biological effectiveness
RBE
Linear energy transfer
LET

ABSTRACT

*Background and purpose:* The relative biological effectiveness (RBE) of proton therapy is predicted to vary with the dose-weighted average linear energy transfer ($LET_d$). However, RBE values may substantially vary for different clinical endpoints. Therefore, the aim of this study was to assess the feasibility of relating mean $D{\cdot}LET_d$ parameters to patient toxicity for HNC patients treated with proton therapy.

*Materials and methods:* The delivered physical dose (D) and the voxel-wise product of D and $LET_d$ ($D{\cdot}LET_d$) distributions were calculated for 100 head and neck cancer (HNC) proton therapy patients using our TPS (Raystation v6R). The means and covariance matrix of the accumulated D and $D{\cdot}LET_d$ of all relevant organs-at-risk (OARs) were used to simulate 2.500 data sets of different sizes. For each dataset, an attempt was made to add mean $D{\cdot}LET_d$ parameters to a multivariable NTCP model based on mean D parameters of the same OAR for xerostomia, tube feeding and dysphagia. The likelihood of creating an NTCP model with statistically significant parameters (i.e. power) was calculated as a function of the simulated sample size for various RBE models.

*Results:* The sample size required to have a power of at least 80% to show an independent effect of mean $D{\cdot}LET_d$ parameters on toxicity is over 15,000 patients for all toxicities.

*Conclusion:* For current clinical practice, it is not feasible to directly model NTCP with both mean D and mean $D{\cdot}LET_d$ of OARs. These findings should not be interpreted as a contradiction of previous evidence for the relationship between RBE and $LET_d$.



The biological damage of proton therapy is generally considered to be higher than that of conventional X-ray radiotherapy of the same physical dose for tumors and healthy tissues [1]. Current guidelines recommend a constant relative biological effectiveness (RBE) model equal to 1.1 for clinical proton therapy treatments, meaning the equivalent physical photon dose equals 1.1 times the physical proton dose [2]. The RBE is used to calculate the RBE-weighted dose ($D_{RBE}$) which is the multiplication of physical dose D and RBE. The $D_{RBE}$ has the unit $Gy_{RBE}$ and represents the equivalent photon dose in Gy. However, a large body of preclinical evidence suggests the RBE varies and multiple variable RBE models have been suggested based on the dose-weighted average linear energy transfer ($LET_d$), fraction dose and tissue-specific $\alpha/\beta$ value [3–6].

Better understanding of the role of $LET_d$ is necessary to give patients the best possible radiation treatment in the near future. Several recent studies have shown the benefit of integrating $LET_d$ into treatment planning optimization in terms of RBE-weighted dose when a variable RBE model is assumed [7–11]. Once these tools become available in commercial treatment planning systems (TPS), treatment planners will have the ability to manipulate the clinical $LET_d$ distribution. Consequently, clinically validated variable RBE models will be required to decide between planning strategies with different $LET_d$ and dose distributions [12].

The evidence for the variability of RBE for in-vitro cell kill is convincing. However, the RBE for cell kill is not necessarily equivalent to the RBE for clinically relevant endpoints such as patient toxicity [12]. Therefore, a recent report by the American Association of Physics in Medicine recommended that variable RBE models need to be cross-validated against clinically relevant endpoints before introduction into clinical treatment planning and optimization [12]. Previous in-patients retrospective investigations showed that the formation of contrast-enhancing brain lesions visible on

* Corresponding author at: P.O.Box 30.0001, 9700 RB Groningen, Groningen, the Netherlands.
*E-mail address:* ir.d.wagenaar@gmail.com (D. Wagenaar).

https://doi.org/10.1016/j.radonc.2021.09.003
0167-8140/

MRI were independently related to both dose (D) and the voxel-wise product of D and $LET_d$, ($D{\cdot}LET_d$) [13,14]. The contribution of $D{\cdot}LET_d$ to contrast-enhancing brain lesions was in agreement with predictions from an existing variable RBE model [5,13]. While contrast-enhancing brain lesions may be considered an adverse event, they are not typically accompanied by clinical symptoms. This indicates that while this endpoint might be a useful surrogate, it is not a clinically relevant outcome itself.

Treatment of head and neck cancer (HNC) typically involves the irradiation of several healthy tissues and organs-at-risk (OARs), as these are often in close proximity to the tumor. Therefore, HNC patients commonly suffer from multiple radiotherapy-induced side effects such as xerostomia, dysphagia and sticky saliva, which can start within the first year of follow-up and may persist for years after treatment [15,16]. In the Netherlands, HNC patients are treated with proton therapy after model-based selection and their toxicities are prospectively scored [17–19]. The effect of RBE variability on HNC toxicity may be studied by combining variable RBE models with normal tissue complication probability (NTCP) models based on X-ray radiotherapy [5,6,15,16].

In short, there is a strong need for validation of variable RBE models for clinically relevant endpoints such as patient toxicity. However, methodologies relating $LET_d$ OAR parameters to patient toxicity are still to be investigated as it is not clear yet if such an analysis would be possible. Therefore, the aim of this study was to assess the feasibility of independently relating the mean $D{\cdot}LET_d$ of OARs to observed patient toxicity for HNC patients treated with proton therapy.

## Materials and methods

### *Study population*

The first 100 consecutive adult HNC patients treated with pencil beam scanning intensity-modulated proton therapy (IMPT) at the University Medical Center Groningen were included in this study. In the Netherlands, patients are selected for proton therapy using a model-based approach. In the model-based clinic, a patient is selected for proton therapy if the ΔNTCP between the proton and photon treatment plans exceeds a certain indication-specific threshold [17]. The ΔNTCP thresholds used for HNC patients are 10% for grade II xerostomia or dysphagia, 15% for the combined total of grade II xerostomia and dysphagia, or 5% for grade III tube feeding dependence [17–19].

Patients were treated with an RBE weighted dose ($D_{RBE}$) of 70 $Gy_{RBE}$ to the primary clinical target volume (CTV) and 54.25 $Gy_{RBE}$ to the prophylactic CTV in 35 fractions with 5 fractions per week using IMPT and assuming a constant RBE of 1.1 (Proteus ®Plus, IBA, Ottignies-Louvain-la-Neuve, Belgium). Patients were immobilized using a 5-point mask (HP Pro, Orfit Industries, Wijnegem, Belgium) and aligned daily using a 6-D robotic table with translations and rotations based on cone-beam CT (CBCT) scans. Potential anatomical changes were monitored with daily online CBCTs and weekly offline verification CTs with the patient immobilized and aligned in treatment position.

Clinical treatment plans were generated using robust optimization employing the treatment planning system (TPS) (RayStation v6 and v9, RaySearch Laboratories, Stockholm, Sweden). Robustness optimization settings were initially a 3% range and 5 mm setup uncertainty which was reduced to a 3 mm setup uncertainty as our clinical experience matured [20]. Target coverage was assessed using the voxel-wise minimum robustness (multi-scenario) evaluation approach, where the coverage criteria was that 95% of the volume of both CTVs should receive at least 98% of the prescribed dose (i.e. $V_{95\%} > 98\%$) in the voxel-wise minimum of all robustness scenarios, as described in a previous publication [21].

### *$LET_d$ calculation and longitudinal dose accumulation*

For the purpose of this study, the $LET_d$ distributions were calculated for protons in a development version of the TPS (RayStation v9R), previously validated for clinical use by our group [22].

The physical dose (D) and $D{\cdot}LET_d$ were calculated on all weekly verification CTs. The $D{\cdot}LET_d$ is the voxel-wise multiplication of dose and $LET_d$ and therefore different form the $LET_d$ itself. The D and $D{\cdot}LET_d$ distributions were deformed to the planning CT and summed to get the accumulated distributions, using the deformable image registration algorithm built into the TPS [23].

### *Dataset simulation and testing*

We simulate the feasibility of relating mean voxel-wise product of D and $LET_d$ ($D{\cdot}LET_d$) of organs-at-risk (OARs) to observed patient toxicity for HNC patients treated with proton therapy in the future. The workflow for simulating and testing datasets is illustrated in Fig. 1. A dataset was gathered of 100 HNC patients including the continuous parameters mean dose (D) and $D{\cdot}LET_d$ for OARs and categorical parameters used in NTCP models (e.g. baseline xerostomia).

Step 1: A multivariate Gaussian distribution was fitted to the continuous parameters determining their standard deviations and covariances. A frequency table was generated for categorical parameters.

Step 2: From the multivariate distribution and frequency table, an unlimited number of realistic patients can be simulated for which the covariance between different continuous parameters is identical to that of the original dataset. A sample size $N$ of up to 100,000 was simulated and each $N$ was simulated 2500 times resulting in 60,000 datasets of various sizes.

Step 3: The RBE-weighted dose ($D_{RBE}$) is calculated assuming a linear RBE model of the form $RBE = 1 + c \cdot LET_d$, where $c$ is the slope of the RBE-$LET_d$ relation so that $D_{RBE} = D + c \cdot D \cdot LET_d$. In our study we performed the analysis for RBE models with different RBE-$LET_d$ slopes. Once with a RBE-$LET_d$ slope $c$ of 0.04 $(keV/\mu m)^{-1}$ as a low estimate which results in a clinical RBE of 1.1 in the target and once with a RBE-$LET_d$ slope $c$ of 0.1 $(keV/\mu m)^{-1}$ as a high estimate, as this value was found in a recent study [13,24].

The $D_{RBE}$ parameters are used to calculate an NTCP-profile based on previously published models for xerostomia, grade 2–4 dysphagia, and tube feeding dependence [15–17]. These NTCP models are based on actual patient toxicity datasets of over 350 photon therapy patients each. The resulting models depend on demographic and $D_{RBE}$ parameters which are summarized in Table 1. Toxicity scores were simulated by assigning a toxicity if the NTCP was higher than a random number drawn from a uniform distribution between 0 and 1 independently for each simulated patient and toxicity.

Step 4: A logistic regression analysis was used to test the hypothesis that the RBE depends on the $LET_d$ in each simulated dataset for each toxicity. For a model consisting of one predicting demographic parameter ($X_{demographic}$) and one dose parameter ($X_D$) the NTCP function is:

$$NTCP(S) = \frac{1}{1 + \exp(-S)} \tag{1}$$

$$S = \beta_0 + \beta_1 \cdot X_{demographic} + \beta_2 \cdot X_D \tag{2}$$

To include a variable RBE, a mean $D{\cdot}LET_d$ parameter is added for each OAR with a mean dose parameter

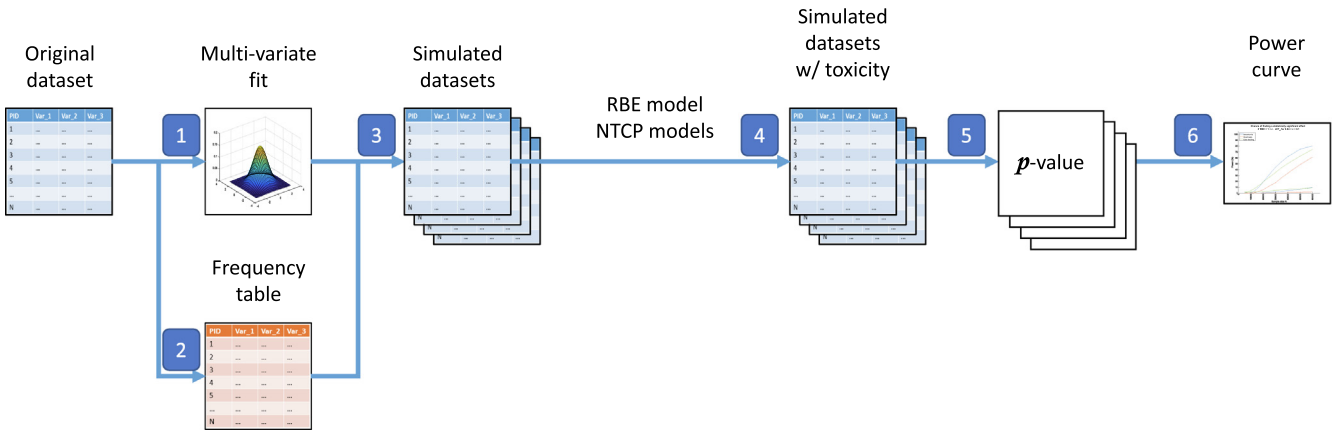


**Fig. 1.** Schematic representation of the workflow for generating and testing datasets. A dataset was gathered of 100 HNC patients including the continuous parameters mean dose (D) and voxel-wise product of D and $LET_d$ ($D{\cdot}LET_d$) for all organs-at-risk and categorical parameters used in NTCP models (e.g. baseline xerostomia). This dataset was used to simulate datasets and estimate the statistical power for various assumed RBE models. See the manuscript text for a detailed explanation of the workflow steps.

**Table 1**
Normal tissue complication models used in this study. These models are taken from the Dutch national proton therapy indication protocol [17]. Using these parameters NTCP is calculated as $NTCP = 1/(1 + \exp(-S))$ where the linear predictor $S$ is defined as $S = \beta_0 + \Sigma\beta_i{\cdot}X_i$.

| Outcome | Parameter | | Estimate |
|---|---|---|---|
| Xerostomia | $\beta_{X0}$ | Intercept | −1.507 |
| | $\beta_{X1}$ | Baseline xerostomia: a bit | 0.525 |
| | $\beta_{X2}$ | Baseline xerostomia: moderate to severe | 1.482 |
| | $\beta_{X3}$ | Mean dose to contralateral parotid gland | 0.052 |
| Dysphagia | $\beta_{D0}$ | Intercept | −3.303 |
| | $\beta_{D1}$ | Baseline dysphagia grade 2–3 | 0.967 |
| | $\beta_{D2}$ | Mean dose to superior pharyngeal constrictor muscle | 0.024 |
| | $\beta_{D3}$ | Mean dose to oral cavity | 0.024 |
| Tube feeding | $\beta_{T0}$ | Intercept | −6.849 |
| | $\beta_{T1}$ | Tumor stage 3–4 | 0.68 |
| | $\beta_{T2}$ | Weight loss 1–10% | 0.317 |
| | $\beta_{T3}$ | Weight loss > 10% | 1.178 |
| | $\beta_{T4}$ | Modality: Accelerated | 0.198 |
| | $\beta_{T5}$ | Modality: Chemoradiation | 1.716 |
| | $\beta_{T6}$ | Modality: Bioradiation | 1.101 |
| | $\beta_{T7}$ | Mean dose to superior pharyngeal constrictor muscle | 0.030 |
| | $\beta_{T8}$ | Mean dose to inferior pharyngeal constrictor muscle | 0.013 |
| | $\beta_{T9}$ | Mean dose to contralateral parotid gland | 0.022 |
| | $\beta_{T10}$ | Mean dose to cricopharyngeal muscle | 0.008 |

$$S' = \beta_0 + \beta_1 \cdot X_{demographic} + \beta_2 \cdot X_D + c \cdot \beta_2 \cdot X_{D{\cdot}LET_d} \quad (3)$$

The adjusted $S'$-function is identical to $S$ when the RBE-$LET_d$ slope $c$ is 0 (Table 2). Inserting $S'$ into the NTCP function, with the beta values and c as the only free parameters, and fitting to the data results in an estimate and standard error of the RBE-$LET_d$ slope $c$. This procedure allows the refitting of the parameter in the NTCP model as well as the RBE-$LET_d$ slope $c$. Refitting all NTCP parameters eliminates the possibility of model inaccuracies being mistaken for $LET_d$ effects. This procedure adds mean $D{\cdot}LET_d$ parameters of OARs to the linear predictor $S$. This is similar to, but slightly different from, adding a $LET_d$ parameter as an effect moderator on the dose–effect relation of these OARs. When considering the mean $D{\cdot}LET_d$, $LET_d$ is only taken into account in areas where there is dose, which is where it is clinically relevant.

Step 5: These simulations were performed 2500 times for sample sizes up to 100,000 patients for a RBE-$LET_d$ slope $c$ of 0, 0.04 and 0.10 $(keV/\mu m)^{-1}$ as described in the dataset simulation subsection above. The power was defined as the proportion of simulations for which the RBE-$LET_d$ slope $c$ was statistically significantly larger than 0. Statistical testing was done using an alpha (probability of type I error) of 0.05 to test the null-hypothesis that the RBE-$LET_d$ slope is 0.

For 2500 simulations the standard error of the power is at most 1.0%. All analyses were performed in Matlab 2018b. The required computation time for all simulations was 83 hours. All Matlab code was reviewed by the second author (AS) and is included in the supplementary material.

## Results

The mean dose D and mean $D{\cdot}LET_d$ parameters of different OARs of the 100 included patients are shown in Fig. 2 and their demographic characteristics are summarized in Table 3.

The proportion of simulations for which a statistically significant independent relation was found (i.e. power) between toxicity and mean $D{\cdot}LET_d$ for OARs is shown in Fig. 3. For a sample size of 5000 patients, the maximum power was 22%. For an assumed RBE-$LET_d$ slope $c$ of 0.10 $(keV/\mu m)^{-1}$, the required number of patients to reach 80% power was 28568, 30,000 and 24,058 for xerostomia, dysphagia and tube feeding respectively. For a RBE-$LET_d$ slope $c$ of 0.04 $(keV/\mu m)^{-1}$, none of the toxicities reached 80% power in our simulations.

For simulations with a RBE-$LET_d$ slope $c$ of 0 $(keV/\mu m)^{-1}$, the power was found to be 6.8%, 9.5% and 24.4% for xerostomia, dysphagia and tube feeding respectively with no clear dependence on sample size (Supplementary materials fig. S1).

When the alpha was increased from 0.05 to 0.10 and testing was performed one-tailed instead of two-tailed, the required number of patients was decreased to 15,120, 17,350 and 14,341 for xerostomia, dysphagia and tube feeding respectively for a RBE-$LET_d$ slope $c$ of 0.10 $(keV/\mu m)^{-1}$ and 85,000, >100,000 and >100,000 respectively for a RBE-$LET_d$ slope $c$ of 0.04 $(keV/\mu m)^{-1}$.

## Discussion

The number of patients required to independently relate the mean $D{\cdot}LET_d$ of OARs to patient toxicity was found to be unfeasibly high for all considered toxicities. Even for 10,000 patients, the power was below 10% for all considered toxicities. This result was confirmed even when the alpha was increased to 0.10 and testing was performed one-tailed.

These results indicate that an independent association between the mean $D{\cdot}LET_d$ of OARs and patient toxicity is unlikely to be pro-

**Table 2**
Definitions of the S′ functions for all normal tissue complication probability models. The normal tissue complication probability can be calculated from these linear predictor functions using formula (1). The demographic parameters were categorized as described by Langendijk et al. [17].

| Model | S-functions |
|---|---|
| Xerostomia | |
| $S' = \beta_{X0} + \beta_{X1} \cdot [base\ xer = 1] + \beta_2 \cdot [base\ xer \geq 2] + \beta_3 \cdot D_{pg\ contra} + c \cdot \beta_3 \cdot DLET_{pg\ contra}$ | |
| Dysphagia | |
| $S' = \beta_{D0} + \beta_{D1} \cdot [base\ dys \geq 2] + \beta_{D2} \cdot D_{pcm\ superior} + \beta_{D3} \cdot D_{oral\ cavity} + c \cdot (\beta_{D2} \cdot DLET_{pcm\ superior} + \beta_{D3} \cdot DLET_{oral\ cavity})$ | |
| Tube feeding | |
| $S' = \beta_{T0} + \beta_{T1} \cdot [T - stage \geq 3] + \beta_{T2} \cdot [1 \leq Weight\ loss \leq 10\%] + \beta_{T3} \cdot [Weight\ loss > 10\%]$ $+\beta_{T4} \cdot [Modality = Accelarated] + \beta_{T5} \cdot [Modality = Chemoradiation]$ $+\beta_{T6} \cdot [Modality = Bioradiation] + \beta_{T7} \cdot D_{pcm\ superior} + \beta_{T8} \cdot D_{pcm\ inferior}$ $+\beta_{T9} \cdot D_{pg\ contra} + \beta_{T10} \cdot D_{cpm} + c \cdot (\beta_{T7} \cdot DLET_{pcm\ superior} + \beta_{T8} \cdot DLET_{pcm\ inferior}$ $+\beta_{T9} \cdot DLET_{pg\ contra} + \beta_{T10} \cdot DLET_{cpm})$ | |
| Base xer: Baseline Xerostomia score on a 4-point scale where 0 is 'none', 1 is 'a little', 2 is 'moderate' and 3 is 'severe'. | |
| Base dys: Baseline dysphagia grade scored between 0 and 4. | |
| Pcm: pharynx constrictor muscle. | |
| Pg contra: The parotid gland contralateral to the target. | |
| Cpm: Cricopharyngeal muscle | |

ven for the considered patient population. This also indicates that estimating the RBE from our current 100 patients would be very inaccurate. There have been previous publications relating patient toxicity to the $D_{RBE}$ calculated using a variable RBE [25,26]. One such study, showed that the observed rib fracture rate after proton therapy of 6.4% for 203 breast cancer patients was in better agreement with photon therapy dose–response relations when considering a variable RBE than with a constant RBE of 1.1 [26]. However, they did not show whether rib fractures were more likely to occur in ribs with higher $LET_d$. As a result, other factors may have contributed to the difference in observed rib fracture rates between photons and protons. For example, many rib fractures are asymptomatic, so that their observed rates are greatly influenced by follow-up procedures which can be different between proton and photon therapy [27]. Another study observed rib-fracture rates up to 18% in breast cancer patients who had undergone radiotherapy when evaluating bone scans every 12 months for at least three years [27]. Even so, the relation between $LET_d$ and rib fracture is of potential interest as higher $LET_d$ can be expected in the ribs. Additionally, rib fracture is a clinical toxicity which is likely to be related to the maximum $D_{RBE}$ which possibly has less correlation with the mean $D{\cdot}LET_d$ of OARs. Therefore, gathering the required sample size to formulate an NTCP model for rib fractures based on both mean D and mean $D{\cdot}LET_d$ for OARs might still be feasible.

Another way to investigate the relation between RBE and $LET_d$ in patients treated with proton therapy may be to consider a different endpoint. Several studies considered the relation between imaging changes and $LET_d$ at voxel level as an objective measure of biological damage which provides more spatial information on the damage [14,28–30]. One such study by Bahn et al. analyzed 110 low-grade glioma patients with 67 contrast-enhancing brain lesions on follow-up MRI scans [13]. They found that the probability of lesions in a voxel was independently related to physical dose, $D{\cdot}LET_d$ and proximity to the ventricular system. The fit parameters estimate an RBE-$LET_d$ slope of 0.1 $(keV/\mu m)^{-1}$, a rate consistent with a variable RBE model with an $\alpha/\beta$ value of 2.0 Gy [5,13]. Another study by Peeler et al. investigated a cohort of 34 pediatric patients treated for ependymoma of which 14 showed hyperintensity on T2-FLAIR MRI scans. They related imaging change probability to physical dose and track-averaged linear energy transfer, but not to $D{\cdot}LET_d$ [30].

These studies show the potential of imaging to provide clinical evidence for the dependency of RBE on $LET_d$. New imaging techniques may be even better suited to investigate RBE variations. With clinically used MRI scans, imaging changes are a dichotomous endpoint (i.e. changes are or are not observed). Diffusion tensor imaging (DTI) is an MRI technique able to detect the anisotropy of water diffusion, which is high in undamaged neural axons. The decrease in DTI values has been related to photon radiotherapy dose and can thus be used to quantify biological damage on a continuous scale [31]. Similarly, the uptake of prostate specific membrane antigen (PSMA) in a PET scan has been related to salivary gland damage and may help localize salivary gland damage [32]. If imaging techniques are able to quantify localized biological damage, each voxel's biological damage can be related to localized dose and $LET_d$ at different time points and in different organs-at-risk.

We found a higher than expected false positive rate for simulations with a RBE-$LET_d$ slope $c$ of 0. The false-positive rate was higher for NTCP models with more independent predictors. The larger number of predictors possibly reduced the accuracy of the model. The large false positive rate indicates the model tests may not have been conservative enough. As a consequence, the actual required number of patients could be higher, not lower. Therefore, this limitation impacts the accuracy of our estimated required sample size but does not impact the conclusions of this study.

An important drawback of looking for evidence of RBE variability using imaging changes is that the endpoints are potentially less clinically relevant than patient toxicity. Our results show that using patient toxicity as an endpoint is not feasible for current clinical practice due to the high correlation between mean physical dose and mean $D{\cdot}LET_d$ for the relevant OARs. This correlation is a consequence of a lack of variation in OAR $LET_d$ caused by similarities in beam setup between patients.

To our knowledge, this is the first study to investigate whether we can expect to find evidence of RBE variability (i.e. using $LET_d$ during the clinical treatment planning process) from future analyses when more patients have been treated with proton therapy. However, some limitations of our study have to be taken into consideration. We limited our study to HNC patients only. A drawback of our approach is that it depends on accurate NTCP models which are not available for all toxicities. We expect the results of our current study in HNC to be valid for toxicities of other treatment sites which depend on mean OAR dose as we expect a similar correlation between mean D and mean $D{\cdot}LET_d$ in OAR, however this was not investigated in our study. We only considered two variable RBE models (i.e. a linear dependency on $LET_d$ with two different RBE-$LET_d$ slopes $c$). While the calculation time would allow for

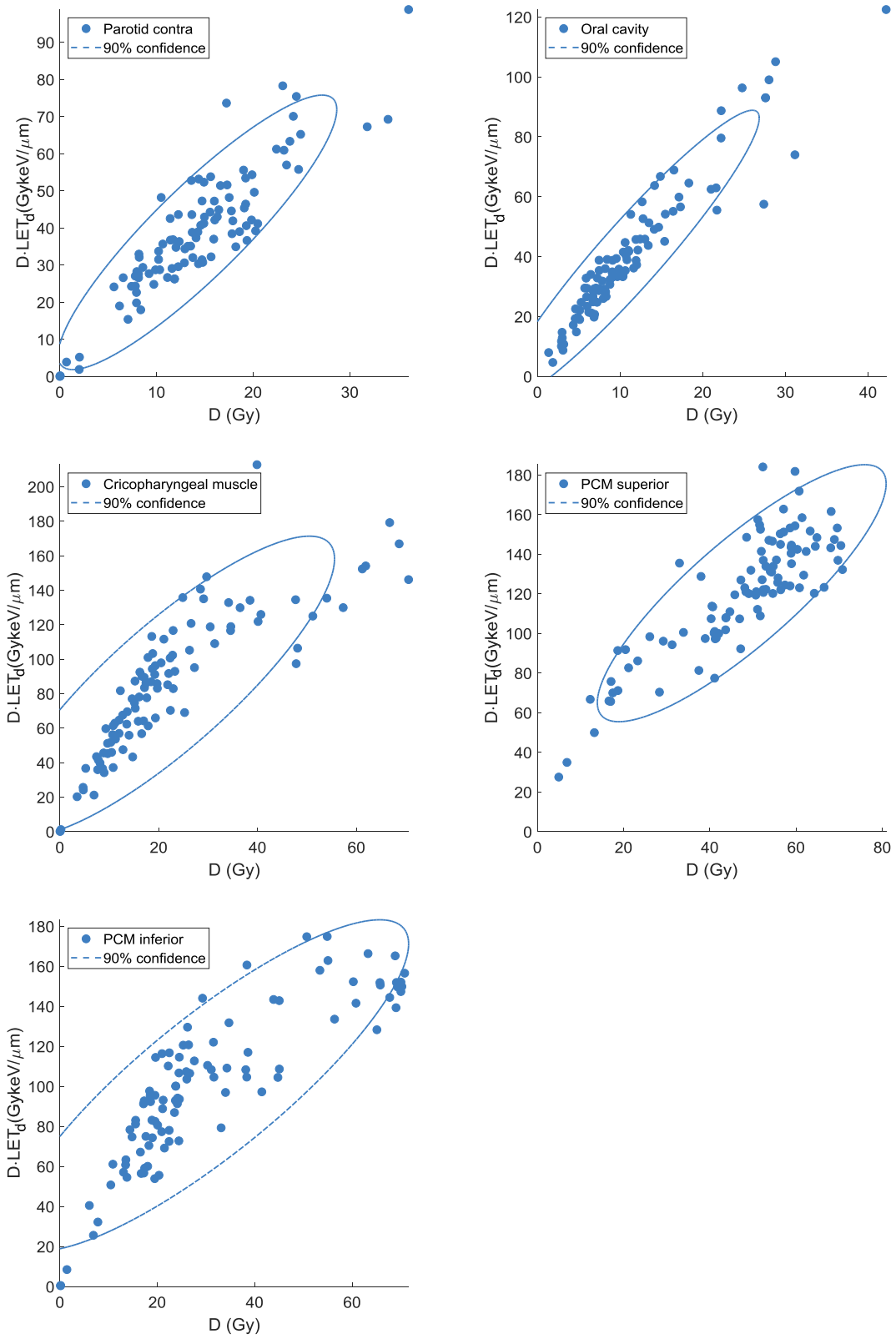


**Fig. 2.** Distributions of mean dose D and voxel-wise product of D and $LET_d$ (D·$LET_d$) to organs-at-risk for head and neck cancer patients treated with proton therapy ($N$ = 100) The line plot represents the 90%-confidence threshold of the two-dimensional Gaussian fit. The Pearson correlations were 0.90 for the contralateral parotid, 0.95 for the oral cavity, 0.85 for the cricopharyngeal muscle, 0.85 for the superior pharynx constrictor muscle and 0.85 for the inferior pharynx constrictor muscle.

more RBE models with intermediate RBE-$LET_d$ slopes to be included, this was unnecessary as the results based on the strongest dependency on $LET_d$ have already indicated an unfeasibly high required patient sample size. In our study the dosimetric parameters were described using a multivariate Gaussian distribution while some non-normality could be present and heteroscedasticity can be observed in Fig. 2. The power for simulations with no RBE-LET relation were higher than the alpha of 5%, indicating that the

**Table 3**
Demographic characteristics of the patient population ($N$ = 100).

| Characteristic | Frequency |
|---|---|
| T-stage | |
| T1–T2 | 34 |
| T3–T4 | 66 |
| Baseline xerostomia | |
| None | 59 |
| A bit | 27 |
| Moderate-severe | 14 |
| Weight loss | |
| None | 55 |
| 1–10% | 27 |
| >10% | 18 |
| Modality | |
| Conventional RT | 23 |
| Accelerated RT | 35 |
| Chemoradiation | 8 |
| Bioradiation | 34 |
| Baseline dysphagia | |
| Grade 0–1 | 60 |
| Grade 2–3 | 40 |
| NTCP | Mean (%) |
| Xerostomia | 40.3 |
| Dysphagia | 20.7 |
| Tube feeding dependence | 6.1 |

The demographic characteristics were scored according with the Dutch National indication protocol [17].

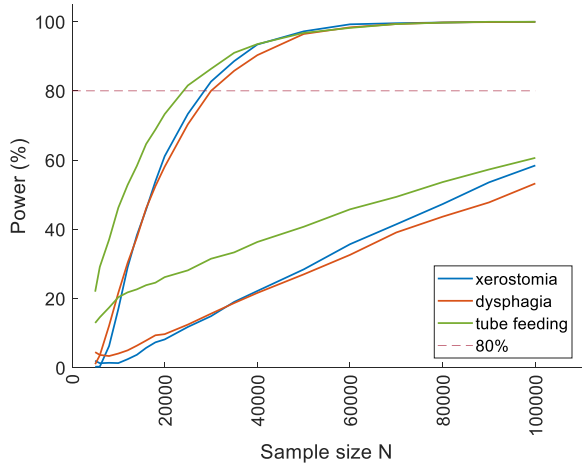


**Fig. 3.** Statistical power of showing an independent relation between toxicity and voxel-wise product of D and $LET_d$ ($D{\cdot}LET_d$) for an assumed RBE-$LET_d$ slope $c$ of 0.04 or 0.1 $(keV/\mu m)^{-1}$. Each toxicity has two line plots associated with it. The lower and higher estimates were for 0.04 and 0.1 $(keV/\mu m)^{-1}$ respectively.

testing methodology may not have been conservative enough and the number of required patients may have been underestimated.

## Conclusions

We conclude that directly relating radiation-induced toxicity to the mean $D{\cdot}LET_d$ of OARs will not be feasible for HNC patients treated with proton therapy in current clinical practice. Future research could focus on the indirect relation between RBE and $LET_d$ through imaging changes using different imaging modalities as these can be used to consider the local dose instead of the mean OAR dose. The presented study in no way contradicts evidence for an increased RBE at the end of proton range. Even though no relation between mean $D{\cdot}LET_d$ for OARs and radiation-induced toxicity is expected to be observed for HNC patients, the incease of RBE is is substantiated by a large body of preclinical evidence. The question how proton RBE exactly depends on $LET_d$ for toxicity is still relevant because it can confirm how $LET_d$ can be used for treatment plan evaluation and will help guide the future implementation of $LET_d$ optimization. Therefore, new methodologies to investigate the proton RBE for clinical endpoints need to be explored.

## Conflict of interest statement

- A research collaboration exists between the Department of Radiation Oncology, University Medical Center Groningen, University of Groningen, Groningen, the Netherlands and the following entities
  - o IBA (Ottignies-Louvain-la-Neuve, Belgium)
  - o Philips (Eindhoven, the Netherlands)
  - o Mirada Medical (Oxford, England)
  - o RaySearch Laboratories (Stockholm, Sweden)
  - o Elekta (Stockholm, Sweden)
  - o Siemens (Munich, Germany)
- The fourth author (JL) reports honorarium for consultancy paid to UMCG Research BV.

## Acknowledgements

We would like to acknowledge the contributions of Gijs Katgert, Nísia Santos Fernandez and Chioma Onyia towards gathering the required data.

## Appendix A. Supplementary data

Supplementary data to this article can be found online at https://doi.org/10.1016/j.radonc.2021.09.003.

## References

[1] Paganetti H, Niemierko A, Ancukiewicz M, Gerweck LE, Goitein M, Loeffler JS, et al. Relative biological effectiveness (RBE) values for proton beam therapy. Int J Radiat Oncol 2002;53:407–21. https://doi.org/10.1016/S0360-3016(02)02754-2.
[2] ICRU. Prescribing, Recording, and Reporting Proton-Beam. ICRU Report 78. vol. 7. 2007. 10.1093/jicru/ndi004.
[3] Paganetti H. Relative biological effectiveness (RBE) values for proton beam therapy. Variations as a function of biological endpoint, dose, and linear energy transfer. Phys Med Biol 2014;59:R419–72. https://doi.org/10.1088/0031-9155/59/22/R419.
[4] Rørvik E, Fjæra LF, Dahle TJ, Dale JE, Engeseth GM, Stokkevåg CH, et al. Exploration and application of phenomenological RBE models for proton therapy. Phys Med Biol 2018;63:185013. https://doi.org/10.1088/1361-6560/aad9db.
[5] Wedenberg M, Lind BK, Hårdemark B. A model for the relative biological effectiveness of protons: the tissue specific parameter α/β of photons is a predictor for the sensitivity to LET changes. Acta Oncol 2013;52:580–8. https://doi.org/10.3109/0284186X.2012.705892.
[6] McNamara AL, Schuemann J, Paganetti H. A phenomenological relative biological effectiveness (RBE) model for proton therapy based on all published in vitro cell survival data. Phys Med Biol 2015;60:8399–416. https://doi.org/10.1088/0031-9155/60/21/8399.
[7] Traneus E, Ödén J. Introducing proton track-end objectives in intensity modulated proton therapy optimization to reduce linear energy transfer and relative biological effectiveness in critical structures. Int J Radiat Oncol 2019;103:747–57. https://doi.org/10.1016/j.ijrobp.2018.10.031.
[8] Unkelbach J, Botas P, Giantsoudi D, Gorissen BL, Paganetti H. Reoptimization of intensity modulated proton therapy plans based on linear energy transfer. Int J Radiat Oncol Biol Phys 2016;96:1097–106. https://doi.org/10.1016/j.ijrobp.2016.08.038.
[9] Cao W, Lim GJ, Lee A, Li Y, Liu W, Ronald Zhu X, et al. Uncertainty incorporated beam angle optimization for IMPT treatment planning. Med Phys 2012;39:5248–56. https://doi.org/10.1118/1.4737870.
[10] Liu C, Patel SH, Shan J, Schild SE, Vargas CE, Wong WW, et al. Robust optimization for intensity modulated proton therapy to redistribute high linear energy transfer from nearby critical organs to tumors in head and neck

cancer. Int J Radiat Oncol 2020;107:181–93. https://doi.org/10.1016/j.ijrobp.2020.01.013.
[11] Bai X, Lim G, Grosshans D, Mohan R, Cao W. A biological effect-guided optimization approach using beam distal-edge avoidance for intensity-modulated proton therapy. Med Phys 2020;47:3816–25. https://doi.org/10.1002/mp.v47.910.1002/mp.14335.
[12] Paganetti H, Blakely E, Carabe-Fernandez A, Carlson DJ, Das IJ, Dong L, et al. Report of the AAPM TG-256 on the relative biological effectiveness of proton beams in radiation therapy. Med Phys 2019;46:e53–78. https://doi.org/10.1002/mp.13390.
[13] Bahn E, Bauer J, Harrabi S, Herfarth K, Debus JJ, Alber M. Late contrast enhancing brain lesions in proton treated low-grade glioma patients: clinical evidence for increased periventricular sensitivity and variable RBE. Int J Radiat Oncol Biol Phys 2020;107:571–8. https://doi.org/10.1016/j.ijrobp.2020.03.013.
[14] Eulitz J, Troost EGC, Raschke F, Schulz E, Lutz B, Dutz A, et al. Predicting late magnetic resonance image changes in glioma patients after proton therapy. Acta Oncol (Madr) 2019;58:1536–9. https://doi.org/10.1080/0284186X.2019.1631477.
[15] Christianen MEMC, Schilstra C, Beetz I, Muijs CT, Chouvalova O, Burlage FR, et al. Predictive modelling for swallowing dysfunction after primary (chemo) radiation: results of a prospective observational study. Radiother Oncol 2012;105:107–14. https://doi.org/10.1016/j.radonc.2011.08.009.
[16] Beetz I, Schilstra C, van der Schaaf A, van den Heuvel ER, Doornaert P, van Luijk P, et al. NTCP models for patient-rated xerostomia and sticky saliva after treatment with intensity modulated radiotherapy for head and neck cancer: the role of dosimetric and clinical factors. Radiother Oncol 2012;105:101–6. https://doi.org/10.1016/j.radonc.2012.03.004.
[17] Landelijk Platform Protonentherapie, Protonentherapie LP. Landelijk Indicatie Protocol Protonen Therapie Hoofd-halstumoren. 2017.
[18] Langendijk JA, Boersma LJ, Rasch CRN, van Vulpen M, Reitsma JB, van der Schaaf A, et al. Clinical trial strategies to compare protons with photons. Semin Radiat Oncol 2018;28:79–87. https://doi.org/10.1016/j.semradonc.2017.11.008.
[19] Tambas M, Steenbakkers RJHM, van der Laan HP, Wolters AM, Kierkels RGJ, Scandurra D, et al. First experience with model-based selection of head and neck cancer patients for proton therapy. Radiother Oncol 2020;151:206–13. https://doi.org/10.1016/j.radonc.2020.07.056.
[20] Wagenaar D, Kierkels RGJ, van der Schaaf A, Meijers A, Scandurra D, Sijtsema NM, et al. Head and neck IMPT probabilistic dose accumulation: Feasibility of a 2 mm setup uncertainty setting. Radiother Oncol 2021;154:45–52. https://doi.org/10.1016/j.radonc.2020.09.001.
[21] Korevaar EW, Habraken SJM, Scandurra D, Kierkels RGJ, Unipan M, Eenink MGC, et al. Practical robustness evaluation in radiotherapy - A photon and proton-proof alternative to PTV-based plan evaluation. Radiother Oncol 2019;141:267–74. https://doi.org/10.1016/j.radonc.2019.08.005.
[22] Wagenaar D, Tran LT, Meijers A, Marmitt GG, Souris K, Bolst D, et al. Validation of linear energy transfer computed in a Monte Carlo dose engine of a commercial treatment planning system. Phys Med Biol 2020;65:025006. https://doi.org/10.1088/1361-6560/ab5e97.
[23] Weistrand O, Svensson S. The ANACONDA algorithm for deformable image registration in radiotherapy. Med Phys 2015;42:40–53. https://doi.org/10.1118/1.4894702.
[24] Unkelbach J, Chan TCY, Bortfeld T. Accounting for range uncertainties in the optimization of intensity modulated proton therapy. Phys Med Biol 2007;52:2755–73. https://doi.org/10.1088/0031-9155/52/10/009.
[25] Ödén J, Toma-Dasu I, Witt Nyström P, Traneus E, Dasu A. Spatial correlation of linear energy transfer and relative biological effectiveness with suspected treatment-related toxicities following proton therapy for intracranial tumors. Med Phys 2020;47:342–51. https://doi.org/10.1002/mp.13911.
[26] Wang C-C, McNamara AL, Shin J, Schuemann J, Grassberger C, Taghian AG, et al. End-of-range radiobiological effect on rib fractures in patients receiving proton therapy for breast cancer. Int J Radiat Oncol 2020;107:449–54. https://doi.org/10.1016/j.ijrobp.2020.03.012.
[27] Kim DW, Kim SJ, Kim K, Shin KH. Spontaneous rib fractures after breast cancer treatment based on bone scans: comparison of conventional versus hypofractionated radiotherapy. Clin Breast Cancer 2020. https://doi.org/10.1016/j.clbc.2020.07.009.
[28] Giantsoudi D, Grassberger C, Craft D, Niemierko A, Trofimov A, Paganetti H. Linear energy transfer-guided optimization in intensity modulated proton therapy: feasibility study and clinical potential. Int J Radiat Oncol 2013;87:216–22. https://doi.org/10.1016/j.ijrobp.2013.05.013.
[29] Bahn E, Bauer J, Harrabi S, Herfarth K, Debus J, Alber M. Late contrast enhancing brain lesions in proton-treated patients with low-grade glioma: clinical evidence for increased periventricular sensitivity and variable RBE. Int J Radiat Oncol Biol Phys 2020;107:571–8. https://doi.org/10.1016/j.ijrobp.2020.03.013.
[30] Peeler CR, Mirkovic D, Titt U, Blanchard P, Gunther JR, Mahajan A, et al. Clinical evidence of variable proton biological effectiveness in pediatric patients treated for ependymoma. Radiother Oncol 2016;121:395–401. https://doi.org/10.1016/j.radonc.2016.11.001.
[31] Connor M, Karunamuni R, McDonald C, White N, Pettersson N, Moiseenko V, et al. Dose-dependent white matter damage after brain radiotherapy. Radiother Oncol 2016;121:209–16. https://doi.org/10.1016/j.radonc.2016.10.003.
[32] Mohan V, Vogel WV, Valk GD, de Boer JP, Lam MGEH, de Keizer B. PSMA PET/CT identifies intrapatient variation in salivary gland toxicity from iodine-131 therapy. Mol Imaging 2020;19:153601212093499. 10.1177/1536012120934992.